The *Dictyostelium* Gelation Factor Shares a Putative Actin Binding Site with α-Actinins and Dystrophin and Also Has a Rod Domain Containing Six 100-Residue Motifs That Appear to Have a Cross-beta Conformation

Angelika A. Noegel,* Susanne Rapp,* Friedrich Lottspeich,‡ Michael Schleicher,* and Murray Stewart§

Max-Planck-Institut für *Biochemie and ‡Genzentrum, 8033 Martinsried, Federal Republic of Germany; and §Medical Research Council Laboratory of Molecular Biology, Cambridge, CB2 2QH, England

Abstract. The 120-kD gelation factor and α-actinin are among the most abundant F-actin cross-linking proteins in *Dictyostelium discoideum*. Both molecules are homodimers and have extended rod-like configurations that are respectively ~35 and 40 nm long. Here we report the complete cDNA sequence of the 120-kD gelation factor which codes for a protein of 857 amino acids. Its calculated molecular mass is 92.2 kD which is considerably smaller than suggested by its mobility in SDS-PAGE. Analysis of the sequence shows a region that is highly homologous to *D. discoideum* α-actinin, chicken fibroblast α-actinin, and human dystrophin. This conserved domain probably represents an actin binding site that is connected to the rod-forming part of the molecule via a highly charged stretch of amino acids. Whereas the sequence of α-actinin (Noegel, A., W. Witke, and M. Schleicher. 1987. *FEBS [Fed. Eur. Biochem. Soc.] Lett.* 221:391–396) suggests that the extended rod domain of the molecule is based on four spectrin-like repeats with high α-helix potential, the rod domain of the 120-kD gelation factor is constructed from six 100-residue repeats that have a high content of glycine and proline residues and which, in contrast to α-actinin, do not appear to have a high α-helical content. These repeats show a distinctive pattern of regions that have high beta-sheet potential alternating with short zones rich in residues with a high potential for turns. This observation suggests that each 100-residue motif has a cross-beta conformation with approximately nine sheets arranged perpendicular to the long axis of the molecule. In the high beta-potential zones every second residue is often hydrophobic. In a cross-beta structure, this pattern would result in one side of the domain having a surface rich in hydrophobic side chains which could account for the dimerization of the 120-kD gelation factor subunits.

ACTIN-binding proteins are generally thought to influence several key mechanical properties of the cytoskeleton of amoeboid cells such as *Dictyostelium discoideum* and macrophages. Although the precise details of the mechanism by which many of these processes take place has still to be determined, it is clear that cross-linking of actin filaments makes a major contribution to the consistency of the cytoplasm and its modulation (for reviews see Stossel et al., 1985; Pollard and Cooper, 1986). Among the most prominent F-actin cross-linking factors in *D. discoideum* cells are α-actinin (Condeelis and Vahey, 1982; Fechheimer et al., 1982; Brier et al., 1983) and the 120-kD gelation factor (Condeelis et al., 1981, 1982). Both molecules are extended rod-shaped homodimers. Electron microscopy of shadowed material has indicated that the extended structure of α-actinin is probably less flexible than that of the 120-kD gelation factor. One manifestation of this difference in flexibility is the tendency of α-actinin to form actin filament bundles whereas the cross-linking activity of the gelation factor leads to a more three-dimensional meshwork (Condeelis et al., 1984). Another difference between α-actinin and the 120-kD gelation factor is the insensitivity of the latter to calcium ions (Condeelis et al., 1981, 1982), in contrast to the F-actin cross-linking activity of *D. discoideum* α-actinin which is completely inhibited by submicromolar concentrations of free Ca^{2+} (Condeelis and Vahey, 1982; Fechheimer et al., 1982).

Progress has recently been made in understanding structure–function relationships in α-actinin. The molecule is a homodimer with the two chains organized in an antiparallel fashion (Wallraff et al., 1986). Cloning (Noegel et al., 1986; Witke et al., 1986) and sequencing (Witke et al., 1986; Noegel et al., 1987) of the cDNA coding for *D. discoideum* α-actinin indicated that the structural elements involved in regulation by Ca^{2+} probably reside in EF-hand domains at the COOH-terminal ends of each chain. The extended struc-

ture of α-actinin from *D. discoideum* and chicken fibroblasts appears to be based on four spectrin-like repeats ~120 residues long with a high α-helix potential (Baron et al., 1987; Wasenius et al., 1987). Both α-actinins have a region near to their NH_2 terminus in which the sequence is highly homologous to a region in human dystrophin (Hammonds, 1987; Koenig et al., 1988; Schleicher et al., 1988*a*). Studies on isolated peptides from chicken smooth muscle α-actinin (Imamura et al., 1988) and on a bacterially expressed fusion protein of *D. discoideum* α-actinin (Schleicher, M., and A. Noegel, manuscript submitted for publication) indicate that this region has actin-binding activity.

A *D. discoideum* mutant that lacks >99% of its endogenous α-actinin, but which still shows undisturbed cell functions, has recently been isolated and characterized (Wallraff et al., 1986; Schleicher et al., 1988*b*), and an α-actinin minus mutant with similar properties has been constructed by gene disruption (Witke et al., 1987; Noegel and Witke, 1988). The striking failure of these cells to manifest any alterations in cellular function, particularly with respect to cell motility, raises the possibility that there might be considerable redundancy in the regulation of the microfilament system in *Dictyostelium*. It could be that, at the cellular level, several different proteins share functionally equivalent roles and interact in similar ways with actin, even using similar binding sites. To explore this possibility further, we have cloned the cDNA that codes for the *D. discoideum* gelation factor (cDGF).[1] Here we report the complete sequence data and show that the gelation factor and α-actinin share a sequence that appears to be a putative actin binding site. Although their rod-like domains are composed from repeating motifs of similar length, these motifs have a strikingly different amino acid composition and probably have quite different secondary structures.

Materials and Methods

Growth and Development of D. discoideum

D. discoideum strain AX2, clone 214, was used for protein purification and isolation of DNA or RNA. The cells were cultivated axenically in shaken suspensions using 10-liter fermenters (Claviez et al., 1982; Schleicher et al., 1984). For time-course experiments, cells were grown axenically to a density of 3×10^6 cells/ml, washed in Soerensen phosphate buffer, pH 6.0, and allowed to develop at 21°C in the light on Millipore Corp. (Bedford, MA) filters (Newell et al., 1969).

Protein Purification

Actin was prepared from rabbit skeletal muscles as described by Spudich and Watt (1971) and further purified by gel filtration on Sephacryl S300. The 120-kD gelation factor was purified from the soluble fraction of aggregation-competent cells essentially as described for the purification of hisactophilin (Scheel et al., 1989). Proteins were eluted from the DEAE column with a linear gradient of 0–350 mM NaCl (2 × 750 ml). The gelation factor eluted at a salt concentration of ~200 mM and was monitored by immunoblotting (Towbin et al., 1979) and low shear viscometry (MacLean-Fletcher and Pollard, 1980); the appropriate fractions were pooled, proteins precipitated with solid ammonium sulfate (35–60% of saturation), and loaded onto a Sepharose6B-Cl column (2.5 × 100 cm) that was equilibrated in IEDABAP buffer (10 mM imidazol, pH 7.6, 1 mM EGTA, 1 mM DTT, 0.5 mM PMSF, 1 mM benzamidine, 0.1 mM ATP, 0.02% NaN_3) containing 0.6 M KCl and primed with IEDABAP buffer plus 0.6 M KI essentially as described (Pollard et al., 1974). Fractions containing gelation factor were dialyzed against MEDABAP buffer (10 mM MES, pH 6.5, 1 mM EGTA, 0.1 mM DTT, 0.02% NaN_3, 1 mM benzamidine, 0.5 mM PMSF, 0.1 mM ATP), loaded onto a hydroxylapatite column (2.5 × 4 cm, equilibrated in MEDABAP buffer), and eluted with a shallow gradient of 0–150 mM potassium phosphate in MEDABAP buffer (2 × 125 ml). For final purification, the protein was chromatographed on a FPLC system (Pharmacia Fine Chemicals, Piscataway, NJ) using a MonoQ column equilibrated in buffer A (30 mM Tris-HCl, pH 7.8, 0.1 mM EGTA, 75 μM DTT, 0.02% NaN_3). In a linear gradient with buffer B (buffer A + 0.5 M NaCl) the protein was eluted at a salt concentration of 280 mM NaCl.

Protein Sequencing

Purified gelation factor was dialyzed against 10 mM ammonium bicarbonate, pH 7.8, and lyophilized. 800 μg of protein was dissolved in 80% formic acid and incubated with 10% (wt/vol) cyanogen bromide for 18 h at 22°C in the dark. After removal of the cyanogen bromide by repeated lyophilization, the degree of cleavage was checked by electrophoresis on 18% acrylamide–SDS gels. The presence of peptides with apparent molecular masses >40 kD suggested incomplete cleavage or long polypeptides without methionine residues. Therefore, 600 μg of the material was digested with 12 μg *N*-tosyl-L-phenylalanine chloromethyl ketone–treated trypsin (Worthington Biochemical Corp., Freehold, NJ) at 37°C in 500 μl of 100 mM ammonium bicarbonate, pH 7.9. The resulting peptides were separated and rechromatographed by HPLC on a C18 reversed-phase column using 0.1% trifluoroacetic acid and 0.1% trifluoroacetic acid in acetonitrile as elution solvents. The amino-terminal sequences of selected peptides were determined on a gas phase sequenator (model 470A; Applied Biosystems, Inc., Foster City, CA) using the program 02npth. The phenylthiohydantoin derivatives were analyzed isocratically by a HPLC system (Lottspeich, 1985). The repetitive yields were 92–96%.

Production of Monoclonal Antibodies

Female Balb/c mice were immunized with purified gelation factor mixed with either Freund's adjuvant or aluminum hydroxide (Serva Feinbiochemica GmbH, Heidelberg) essentially as described (Schleicher et al., 1984). Production and characterization of the monoclonal antibodies will be described elsewhere.

DNA Isolation and Hybridization Analysis

D. discoideum chromosomal DNA was isolated from purified nuclei (Noegel et al., 1985) and digested with Hind III. The restriction fragments were separated on agarose gels and transferred to nitrocellulose essentially as described by André et al. (1988). A 279-bp Hinf I fragment that coded for most of the putative actin binding site was isolated from the *D. discoideum* α-actinin gene, nick translated, and used as a probe under low stringency conditions (30% formamide, 2× standard saline citrate, 1% Sarkosyl, 4 mM EDTA, 0.1% SDS, 4× Denhardt's solution, and 0.12 M sodium phosphate buffer, pH 6.8, at 37°C for 18 h). For comparison, a gelation factor–specific probe of cDGF10 (bp 1–1,501) was nick translated and hybridized under high stringency conditions (50% formamide).

Isolation of cDNA Clones

A λgt11 cDNA library kindly provided by Drs. R. Kessin and M.-L. Lacombe (Lacombe et al., 1986) (Columbia University, New York) was screened with a mixture of eight different iodinated monoclonal antibodies against the 120-kD gelation factor as described (Noegel et al., 1986). The DNA of 11 different recombinant phages was purified using standard methods (Maniatis et al., 1982), digested with Eco RI, and the resulting fragments separated on a 0.7% agarose gel in Tris–borate buffer, pH 8.3 (Maniatis et al., 1982). The DNA fragments were isolated by electrophoresis onto DE81 paper, eluted from the paper with 1 M LiCl and 20% ethanol in TE buffer (10 mM Tris-HCl, pH 8.0, 1 mM EDTA), and subcloned into Eco RI-digested pUC19 (Yanisch-Perron et al., 1985). The DNA fragments were further characterized by restriction mapping and hybridization analysis.

cDNA Sequencing

The cDNA sequences of three recombinant phages λcDGF4, λcDGF7, and λcDGF10 were determined (cDGF stands for cDNA of the *Dictyostelium*

1. *Abbreviation used in this paper*: cDGF, cDNA of the *Dictyostelium* gelation factor.

Gelation Factor). λcDGF4 harbored one insert of 0.6 kb. λcDGF7 and λcDGF10 harbored three Eco RI fragments each: 0.6, 0.64, and 1.1 kb for λcDGF7; and 0.6, 0.6, and 1.5 kb for λcDGF10. All Eco RI fragments recognized a mRNA species of ~3 kb when they were used as probes in Northern blot analysis of total *D. discoideum* RNA. λcDGF10 with a 2.7-kb insert proved to contain the coding sequence for the complete gelation factor. To clone the complete cDNA inserts of λcDGF7 and λcDGF10 in the plasmid vector pUC19, the phage DNA was digested with Kpn I and Sst I, inserts of ~4 kb were isolated and subcloned into pUC19 which was appropriately cleaved. Kpn I and Sst I do not cleave the cDNA inserts but have recognition sites close to the Eco RI site of λgt11 (Young and Davis, 1983) which was used for cloning during the construction of the cDNA library (Lacombe et al., 1986). The sequence of cDGF4, 7, and 10 and of two exonuclease III/exonuclease VII-generated clones (Henikoff, 1984) was determined in plasmid pUC19 by the chain-termination method (Sanger et al., 1977) using pUC19-specific primers as well as primers derived from the generated sequences. Both strands of the cDNAs were sequenced.

Expression of Gelation Factor Peptides in Escherichia coli

For expression in *E. coli*, the pIMS vector series (Simon et al., 1988), generously given to us by Dr. M. Veron (Pasteur Institute, Paris, France) was used. The pIMS vectors allow the expression of foreign proteins under the control of the lacZ promoter. The DNA can be cloned in three possible reading frames into an Eco RI site which is located behind an ATG start codon. Depending on the reading frame, the fusion proteins generated in these vectors contain only one to three additional amino acids at their amino terminus and their production can be induced by the addition of isopropyl-l-thio-β-D-galactopyranoside. The *E. coli* strain JM83 was used for the expression of fusion proteins. A Ssp I/Sst I fragment of λcDGF10 was cloned into pIMS6 for the expression of the complete gelation factor in *E. coli* JM83 and the transformants were screened in a colony blot assay (Simon et al., 1988) for the expression of the fusion protein. Growth was at 37°C for 3–4 h before induction. The cells were harvested by centrifugation 1 h after induction, frozen in liquid nitrogen, and used for SDS-PAGE followed by immunoblot analysis.

Computer Analysis of the Sequence

The sequence was analyzed using the program packages from the University of Wisconsin Genetic Computer Group (UWGCG; Madison, WI) and the Protein Identification Resource (PIR; National Biochemical Research Foundation, Washington DC). Dot matrix comparisons were performed with the programs Compare and Dotplot (UWGCG; Maizel and Lenk, 1981). Surface probability was investigated with the programs Peptidestructure and Plotstructure (UWGCG) according to the method of Emini et al. (1985). Searches for similarities to other DNA or protein sequences were done with the programs Fastn and Fastp (PIR; Lipman and Pearson, 1985) using the databanks Mipsy and Mipsx (Martinsried Institute for Protein Sequence Data, Martinsried, FRG) which contain the combined entries from all databanks available. Fourier transforms were calculated as described by Stewart and McLachlan (1975), either scoring residues as 0 or 1, or by scoring according to the beta-sheet potentials of Chou and Fasman (1978). Secondary structure predictions were also computed as described by Garnier et al. (1978).

Results

Isolation and Characterization of cDNA Clones

Using a mixture of eight different monoclonal antibodies, 11 clones were isolated from the λgt11 *D. discoideum* cDNA library. The inserts from four of these clones were sequenced following the strategy illustrated in Fig. 1. The size of the gelation factor mRNA was ~3 kb and the message was present throughout the development of *D. discoideum* (André et al., 1988). The DNA sequence and deduced amino acid sequence of the *D. discoideum* gelation factor are shown in Fig. 2. The coding region spanned 2,574 bp and coded for 857 amino acids. The codon usage was in agreement with that seen for other *D. discoideum* genes (Warrick and Spudich,

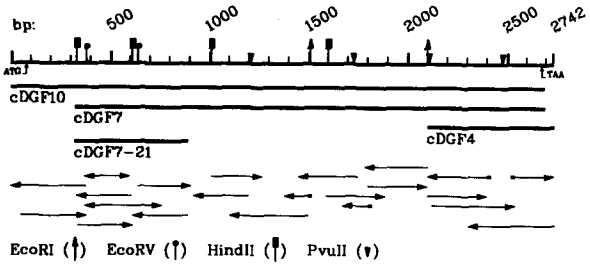

Figure 1. Sequencing strategy of cDGF. The clones cDGF4, 7, and 10 were isolated from recombinant λgt11 phages and their sequences determined by the dideoxy chain-termination method. Sequence information obtained from subcloned restriction enzyme fragments were used to generate specific, synthetic, oligonucleotide primers (*broadened arrow bases*) for completion of the sequence. Only the restriction sites relevant for subcloning are shown.

1988). A polyadenylation signal was identified 23 bp downstream from the TAA stop codon.

On SDS-PAGE the *D. discoideum* gelation factor has an apparent molecular mass of 120 kD (Condeelis et al., 1982). However, the calculated molecular mass of the predicted 857 amino acid sequence was only 92.2 kD, which is even smaller than the molecular mass of α-actinin (97.6 kD; Noegel et al., 1987). Although fibrous proteins are notorious for migrating anomalously in SDS-PAGE (see for example Kaufmann et al., 1984), the magnitude of the discrepancy was such as to question whether the clone λcDGF10 represented the correct as well as complete coding region. We addressed these problems in the following ways.

First, we used highly specific monoclonal antibodies for screening the cDNA expression library, thus reducing the probability of isolating false positive clones; each of the 120-kD-specific monoclonal antibodies alone recognized the λcDGF10-phage plaques (i.e., no epitope was missing). Strong evidence that the material coded for by the cDNA clones was genuinely the gelation factor was obtained from sequence studies of tryptic and cyanogen bromide peptides isolated from the gelation factor prepared from *D. discoideum*. The amino acid sequences of nine such peptides were determined and in all cases matched with the corresponding regions in the deduced amino acid sequence (see Fig. 2). Because the NH_2 terminus of the gelation factor was blocked, we were unable to determine the NH_2-terminal sequence of the protein.

Second, λcDGF10 DNA and genomic AX2 DNA were digested with various restriction enzymes in parallel and analyzed in a Southern blot using cDGF10 DNA as probe. A comparison of the fragment sizes generated with both DNAs indicated the absence of deletions in the cDNA (Fig. 3, *A* and *B*).

Third, we expressed the complete cDNA clone cDGF10 in *E. coli* using the ATG expression vector, pIMS6 (Simon et al., 1988). In immunoblots the fusion protein had the same electrophoretic mobility as the purified 120-kD gelation factor (Fig. 3 *C*). This observation confirmed that the material coded for by the cDNA clone also behaved anomalously in SDS-PAGE and was indistinguishable from genuine gelation factor under these conditions. Possibly, the irregular mobility on SDS gels was due to the highly asymmetric distribution of particular amino acid residues, especially glycine and

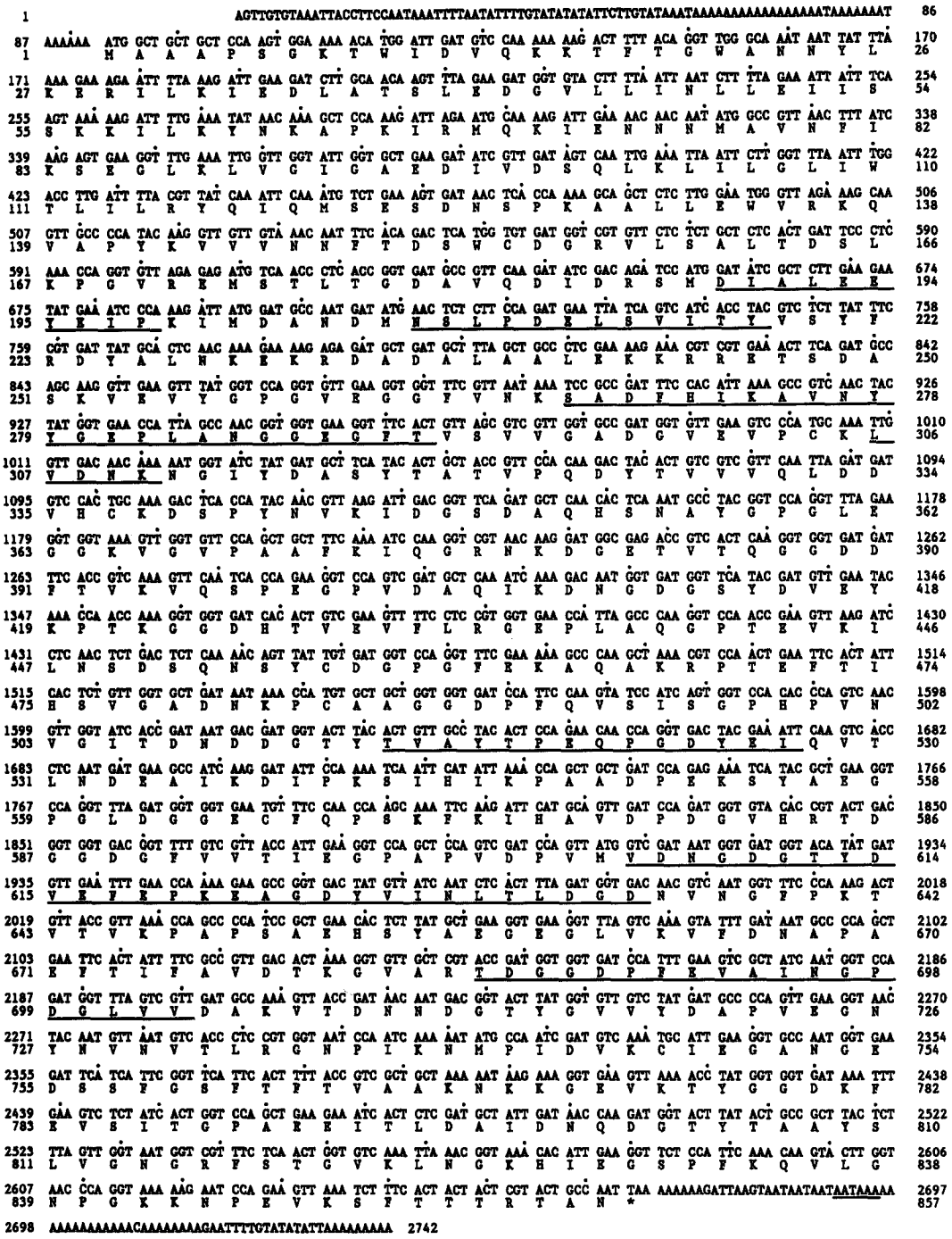

Figure 2. Nucleotide and deduced amino acid sequence of the cDGF. The underlined amino acids denote the peptides which were isolated from purified gelation factor and sequenced in a gas phase sequenator. At the 3′ end, the nucleotide sequence of a polyadenylation signal is underlined.

proline (see Fig. 8). Finally, based on the predicted protein sequence, *D. discoideum* gelation factor should have a net charge of −46, compared to −37 predicted for α-actinin. The more acidic nature of the gelation factor was consistent with the observed relative values of pI 5.5 for α-actinin (Schleicher et al., 1988*b*) and pI 5.3 for gelation factor.

Conserved Actin Binding Site

A Dotplot comparison between *D. discoideum* α-actinin and gelation factor (Fig. 4 *A*) showed a strong homology involving ~250 amino acid residues at the NH_2 termini of both molecules. In *D. discoideum* α-actinin, this region has been shown to exhibit an actin-binding activity (Schleicher, M., and A. Noegel, manuscript submitted for publication) and has been found to be conserved in both chicken fibroblast α-actinin and human dystrophin (Noegel et al., 1987; Schleicher et al., 1988*a*). At the same stringency, a comparison between *D. discoideum* gelation factor and the NH_2-terminal part of human dystrophin (Koenig et al., 1988) also showed a homology of equivalent strength over a sequence of similar length to that seen between *D. discoideum* α-actin-

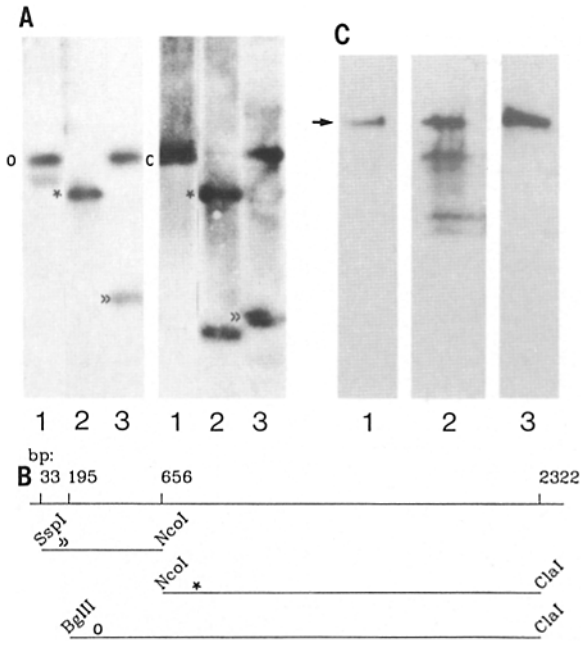

Figure 3. (*A* and *B*) Southern blot analysis of genomic *D. discoideum* DNA using the complete cDNA clone cDGF10 as a probe. *D. discoideum* DNA (*A*, left lanes) and λDGF10 (*A*, right lanes) were digested with the restriction enzymes Bgl II/Cla I (lanes *1*), Nco I/Cla I (lanes 2), and Ssp I/Nco I (lanes *3*). The resulting fragments covered ~85% of the coding region as determined from cDGF10. In the restriction map (*B*) and the autoradiograms the corresponding fragments are labeled with identical symbols. Additional bands are due to hybridization of the complete cDNA probe to neighboring fragments in the genomic or the vector DNA. The nearly identical sizes of the labeled fragments in the genomic and vector DNA indicate that no major deletions have been generated in the cDNA. (*C*) Comparison of the electrophoretic mobilities of *D. discoideum* gelation factor and a cDNA-derived fusion protein. *D. discoideum* homogenate (2×10^5 cells; lane *1*), a homogenate (20 μg protein) of transformed *E. coli* after expression of the complete gelation factor cDNA in the ATG expression vector pIMS (lane 2), and purified gelation factor (2 μg protein) (lane *3*) were separated by SDS-PAGE (10% acrylamide), blotted onto nitrocellulose, probed with a gelation factor–specific monoclonal antibody, and autoradiographed. Although the labeled material from *E. coli* was heavily degraded, the mobility of the largest peptide (*arrow*) that was labeled by the antibody was indistinguishable from that of the genuine *D. discoideum* gelation factor.

in and gelation factor (Fig. 4 *B*). Aligning of the sequences showed highest similarity in the first half of the conserved region. Fig. 4 *C* lists these domains from the *D. discoideum* gelation factor (Fig. 4 *C*, *DG*), *D. discoideum* α-actinin (Fig. 4 *C*, *DA*), chicken fibroblast α-actinin (Fig. 4 *C*, *CA*), and human dystrophin (Fig. 4 *C*, *HD*). Within the homologous regions from *D. discoideum* gelation factor and human dystrophin, 80 out of 107 amino acids were identical or conserved (which we defined as belonging to one of the permutation matrix [PIR] groups: D,E,Q,N; F,Y,W; I,L,V,M; S,T,A,G; or H,R,K).

Southern blot analysis was used to further explore the distribution of proteins containing the putative actin binding site in the *Dictyostelium* genome by probing Hind III–digested *D. discoideum* DNA with a *D. discoideum* α-actinin-specific Hinf I fragment (bp 364–643) that contained the coding region for the putative actin binding site. The digestion with Hind III generates an α-actinin-specific fragment of ~1.2 kb (Witke et al., 1986) which allowed the unequivocal interpretation of the pattern of hybridization. Under low stringency conditions, the α-actinin gene as well as the gene coding for the gelation factor hybridized to the nick-translated probe (Fig. 5, lane *A*). These data indicated that probably only two actin-binding proteins are present in *D. discoideum* that share the same actin binding site with a high degree of similarity. Several very weak bands can be seen under low stringency conditions after overexposure and we can not exclude that additional proteins with mild homologies exist in *D. discoideum*. Under high stringency conditions, a gelation factor–specific probe, that also contained the coding region for the putative actin binding site, did not cross-react with the α-actinin gene (Fig. 5, lane *B*). In addition, Southern blot analysis suggested that the *D. discoideum* genome contains only a single gene coding for the 120-kD gelation factor. Digestion with other restriction enzymes and probing with the complete cDNA gave similar results (data not shown).

The region that connects the putative actin binding site with the repeating units (see Fig. 8, *arrow*) is highly enriched in charged amino acids (KEKRDADALAALEKKRRE) and gave by far the highest values for surface probability calculated according to Emini et al. (1985). Although the mechanism by which the cross-linking function of the gelation factor is regulated has not yet been identified, this region could be a putative regulatory site either for binding to a kinase (e.g., proteinkinase A) or to calmodulin as has been proposed for the regulation of caldesmon (for review see Sobue et al., 1988).

Internal Repeats in the Gelation Factor

Matrix comparison of the sequence of the 120-kD gelation factor with itself indicated the presence of a strong sixfold repeated structure with a repeat length of ~100 residues (Fig. 6 *A*). The dot matrix comparison and the alignment of the six repeats (Fig. 6 *B*) illustrated that there was a very substantial degree of homology between the six individual 100-residue motifs. The homology was greatest in the first five motifs and was weaker in the final motif, at the COOH terminus of the sequence, where it was necessary to introduce a large number of deletions to retain homology. All the motifs were comparatively rich in glycine and proline residues and there were often short sequences in which every second residue had a hydrophobic side chain (Fig. 6 *B*). In these regions the sequence could be written as HxHxHxH . . ., where *H* represented a hydrophobic side chain, whereas *x* was often hydrophilic.

Secondary structure predictions using the method of Garnier et al. (1978) did not suggest that the 100-residue motifs would be high in α-helix, which would be consistent with the large number of proline and glycine residues interspersed throughout the motif. However, the prediction for extended (often beta-sheet) structure showed a quite remarkable oscillation, with a period of ~10 residues (Fig. 7 *A*). We further investigated this feature of the sequence using Fourier analysis, a mathematical technique that is very effective in detecting and evaluating periodic data. Essentially, Fourier analysis expresses a mathematical function in terms of waves (for reviews see McLachlan and Stewart, 1976; Stewart, 1988)

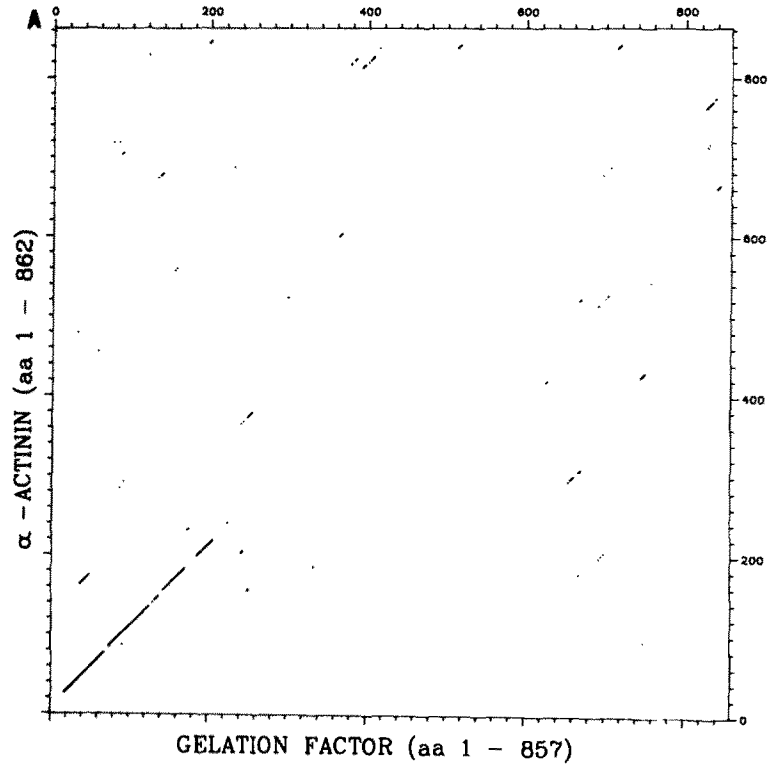

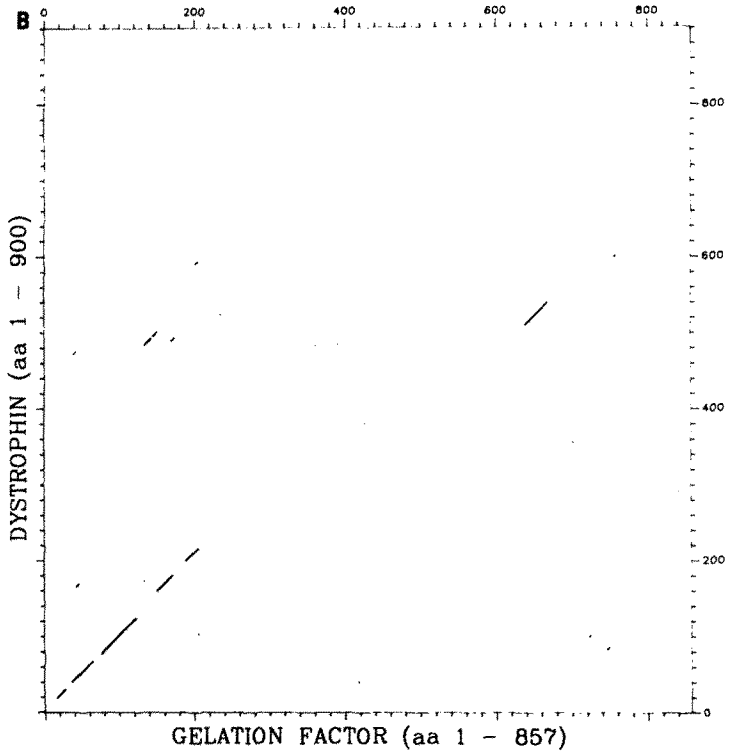

C

```
DG:  7 GKTWIDVQKKTFTGWAN.NYLKERILKIEDLATSLEDGVLLINLLEIISSKKILK 60
DA: 17 NKAWEITQKKTFTAWCN.SHLRKLGSSIEQIDTDFTDGIKLAQLLEVISNDPVFK 70
CA: 27 DPAWEKQQRKTFTAWCN.SHLRKAGTQIENIEEDFRDGLKLMLLLEVISGERLAK 80
HD: 10 CYERERDVQKKTFTKWVNAQFSKFGKQHIENLFSDLQDGRRLLDLLEGLTGQKLPK 64

DG: 61 YNKAPKI.RMQKIENNNMAVNFIKSEGLKLVGIGAEDIVDSQLKLILGLIWTLIL 114
DA: 71 VNKTPKLRRIHNIQNVGLCLKHIESHGVKLVGIGAEELVDKNLKMTLGMIWTIIL 124
CA: 81 PERG.KM.RVHKISNVNKALDFIASKGVKLVSIGAEEIVDGNVKMTLGMIWTIIL 133
HD: 65 .EKGS.T.RVHALNNVNKALRVLQNNNVDLVNIGSTDIVDGNHKLTLGLIWNIIL 116
```

Figure 4. (*A* and *B*) Dotplot analysis of *D. discoideum* gelation factor with *D. discoideum* α-actinin and the NH_2-terminal part of human dystrophin. The comparisons of gelation factor with α-actinin (*A*) and with dystrophin (*B*) show a similarly strong homology between all three proteins in a region of ~250 amino acids. The comparison was generated using the programs Compare and Dotplot (UWGCG). The axes are calibrated in amino acid sequence numbers (window size, 30; stringency, 16). (*C*) Alignment of conserved amino acid sequences from the *D. discoideum* gelation factor (*DG*), *D. discoideum* α-actinin (*DA*), chicken fibroblast α-actinin (*CA*), and human dystrophin (*HD*). Identical residues which are shared by at least three proteins are boxed, the numbers of the amino acids are indicated.

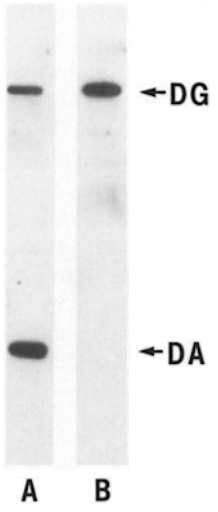

Figure 5. Southern blot analysis of *D. discoideum* DNA under different stringencies. The Hind III–digested *D. discoideum* DNA was probed with an α-^{32}P-labeled Hinf I fragment from the *D. discoideum* α-actinin gene under low stringency (30% formamide). This fragment originates from the region that is highly conserved between *D. discoideum* α-actinin (*DA*) and gelation factor (*DG*), and labels both genes (lane *A*). The fragment sizes are ~1.2 kb (*DA*) and >10 kb (*DG*). In a control experiment, a gelation factor–specific probe was used under high stringency (50% formamide). In this case only the gene that codes for the gelation factor is labeled (lane *B*).

and, if the function is periodic, then only waves corresponding to the repeat distance (or fractions of it) will make a substantial contribution. To analyze the gelation factor in this way, its chemical sequence was transformed into a mathematical sequence by coding the residues according to their Chou and Fasman (1978) beta-forming potential. The Fourier spectrum obtained from the entire 120-kD protein sequence (Fig. 7 *B*) showed a very strong peak at a frequency of 10 residues, which confirmed that the periodic feature seen in Fig. 7 *A* was genuine and gave a more precise estimate of its frequency. In addition, there was also a series of subsiduary peaks at frequencies that were at orders of 100 residues (because the Fourier transform is a spectrum and so is expressed in terms of frequency, which is the reciprocal of the number of residues, the peaks due to a frequency of 100 residues and its overtones are spaced in the spectrum at one tenth the distance apart as the peaks corresponding to 10

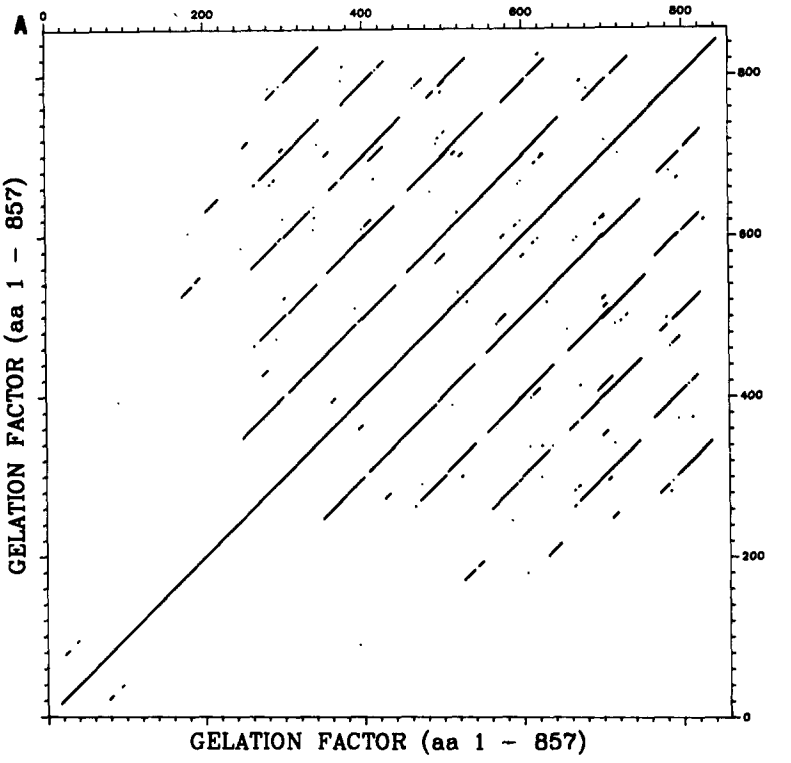

B

REPEAT:

BETA SHEETS:

. . . . . HxHxH . . . . . HxHxH . . . . HxHxH . . . . . HxHxH .

I GPGVEGGFVNKSADFHIKAVNYYGEPLANGGEGFTVSVVGADGVEVPCKLV
II GPGLEGGKVGVPAAFKIQGRNKDGETVTQGGDDFTVKVQSPEG.PVDAQIK
III GPGFEKAQAKRPTEFTIHSVGADNKPCAAGGDPFQVSISGPH..PVNVGIT
IV GPGLDGGECFQPSKFKIHAVDPDGVHRTDGGDGFVVTIEGPA..PVDPVMV
V GEGLVKVFDNAPAEFTIFAVDTKGVARTDGGDPFEVAINGPDGLVVDAKVT
VI GEDSS....FGSFTFTVAAKNKKGEVKTYGGDKFEVSITGPAEEITLDAI.

. . . . . HxHxH . . . . . HxHxHxH . . . . . HxHxH . . . . . .

DNKNGIYDASYTATVPQDYTVVVQLDDVHCKDSPYNVKID.GSDAQHSNAY
DNGDGSYDVEYKPTKGGDHTVEVFLRGEPLAQGPTEVKIL.NSDSQNSYCD
DNDDGTYTVAYTPEQPGDYEIQVTLNDEAIKDIPKSIHIKPAADPEKSYAE
DNGDGTYDVEFEPKEAGDYVINLTLDGDNVNGFPKTVTVKPAPSAEHSYAE
DNNDGTYGVVYDAPVEGNYNVNVTLRGNPIKNMPIDVKCIEG.....AN
DNQDGTYTAAYSLVGNGRFSTGVKLNGKHIEGSPFKQVLGNPGKKNPEVKS

Figure 6. (*A*) Dotplot analysis of *D. discoideum* gelation factor with itself. The comparison shows six very strong repeats at the COOH-terminal part of the molecule. The dotplot was generated using a window size of 30 and a stringency of 16. (*B*) Alignment of the repeats. The repeated units are about 100 amino acids each and start with the amino acid numbers 257 (*I*), 358 (*II*), 458 (*III*), 558 (*IV*), 658 (*V*), and 753 (*VI*). Identical amino acids in three or more of the aligned positions are boxed, the putative beta-sheet regions (see also Fig. 9) are marked with HxHxH.

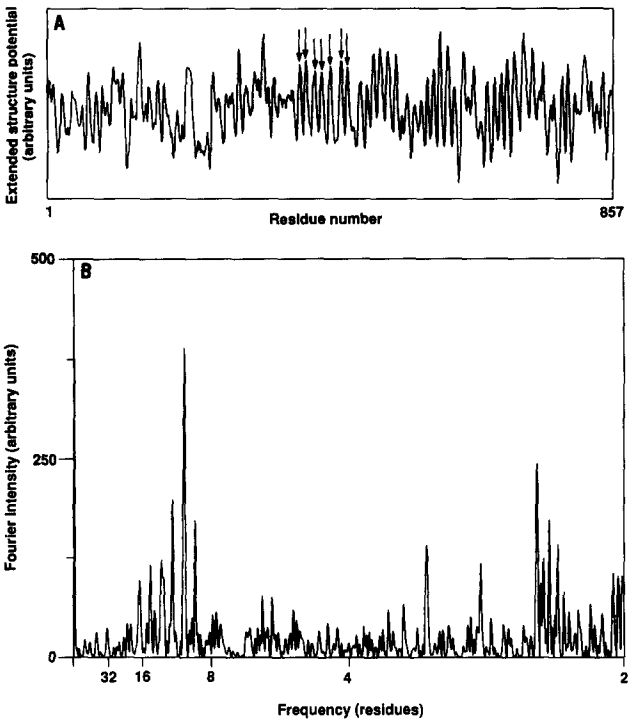

Figure 7. (*A*) Oscillation of beta-sheet structure potential in the rod domain of the gelation factor. The potential for an extended structure computed as described by Garnier et al. (1978) shows a distinctive pattern of successive maxima (*arrows*) and minima with a period of ~10 residues. (*B*) The Fourier spectrum of the Chou and Fasman (1978) beta potential shows a strong peak at a frequency of 1 per 10 residues, confirming the presence of a repeating structure.

residues). We interpret this pattern as deriving from a relatively broad peak centered on a 10-residue frequency that has been sampled by the 100-residue motif repeat. (Such a phenomenon is analogous to the way in which, in a crystal diffraction pattern, the Fourier transform of the repeating unit is sampled by the Fourier transform of the crystal lattice: for reviews see Fraser and MacRae, 1973; Stewart, 1988). A broad underlying peak centered on a frequency of 10 residues would indicate that there was an average repeat in the beta potential of the 100-residue motifs at 10 residues, but that there was considerable variation between repeats which broadened the peak in the same way that loss of long-range order in crystals broadens diffraction peaks (see for example Stewart, 1988). Generally the peaks in the beta potential of the sequence corresponded with the HxHxH zones containing a hydrophobic residue in every second position.

Discussion

We have obtained cDNA clones from a λgt11 library that have been shown by antibody binding, sequencing of tryptic and cyanogen bromide peptides, and by SDS-PAGE mobility of the protein expressed in *E. coli* to correspond to the entire 120-kD gelation factor from *D. discoideum*. Interestingly, the molecular mass of this protein is only 92.2 kD, even lower than that of *D. discoideum* α-actinin which was initially described as a 95-kD protein (Condeelis and Vahey, 1982; Fechheimer et al., 1982) and found to have a molecular mass of 97.6 kD as calculated from the cDNA sequence (Noegel et al., 1987). Numerous, unglycosylated proteins are known that show high discrepancies between apparent molecular masses in SDS-PAGE and calculated molecular masses according to the primary structure. Abnormal electrophoretic mobility often indicates amino acid compositions that differ strongly from the average amino acid frequency in eukaryotic proteins. For example, the tau protein has much higher proportions of glycine (10.2 mol%) and proline (8.8 mol%) residues than the average vertebrate globular protein (Lee et al., 1988) and shows in SDS-PAGE an apparent molecular mass of 47–50 kD which is ~30% higher than expected from the cDNA deduced molecular mass. As shown in Fig. 8, the distribution of glycine and proline residues in the 120-kD subunit is highly asymmetrical. In the region of the 6 × 100 amino acids repeats, the glycine content is 12.8 mol% and the proline content 7.2 mol%. This feature could be the reason for its reduced mobility in SDS gels.

Analysis of the protein sequence of the gelation factor deduced from the cDNA sequence (Fig. 2) revealed a region at the NH_2 terminus that was extremely similar to the proposed actin binding site of *D. discoideum* α-actinin. The presence of the same actin binding site in two proteins from one cell raised the question whether both proteins compete for binding to filaments. According to Carboni and Condeelis (1985), the location and distribution of α-actinin and gelation factor can be distinguished during cell locomotion and chemotaxis. The construction of mutants with multiple defects in actin-binding proteins could clarify this problem.

The homologies of a 250 amino acid region from the NH_2 termini of *D. discoideum* α-actinin, *D. discoideum* gelation factor, chicken fibroblast α-actinin, and human dystrophin suggests an evolutionarily conserved actin binding site. The biochemical function of dystrophin is still unclear, but the presence of a putative actin binding site indicates that dystrophin is an actin-binding protein. In this conserved region, the highest similarity shared by α-actinin, gelation factor, and human dystrophin resides in a stretch of ~100 amino acids (Fig. 4 *C*). In this region, the *D. discoideum* gelation factor and human dystrophin have 41.1% residues in common, which is very close to 46.4% of identity between the *D. discoideum* gelation factor and α-actinin. To gain a greater insight into the mechanism of actin binding, we are currently using selected synthetic peptides to produce monoclonal and polyclonal antibodies that are directed against these conserved sites.

In addition to the putative actin-binding domain, the protein sequence of the gelation factor was also characterized by a distinctive sixfold repeat of 100 residues that most likely corresponded to the rod domain of the molecule (Fig. 6 *A*). Such a feature of the sequence probably arose by a series of gene duplication events. Experience on other fibrous proteins (see Stewart et al., 1989 for a review) suggests that such a repeating feature might also be related in some way to interactions between chains in the molecule or between different molecules. We therefore analyzed the pattern in the repeating 100-residue motif to see if any predictions could be made relating to the conformation, structure, and function of the gelation factor and to assess how similar they were to the repeats of approximately the same size seen in the α-actinin sequence.

Although the 100-residue motif in the 120-kD gelation factor was about the same length as the repeating motif in

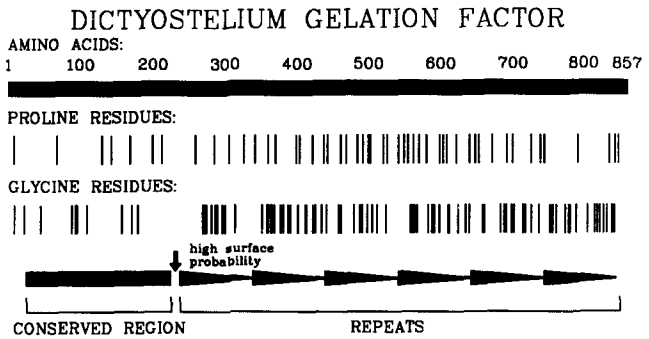

Figure 8. Map of the gelation factor polypeptide structure. The molecule consists of 857 amino acids; the proline and glycine residues are asymmetrically distributed and are clustered in the six-fold repeat region. A highly charged stretch of amino acids connects the putative actin binding site with the repeat region.

spectrin (Speicher and Marchesi, 1984; Speicher, 1986), α-actinin (Baron et al., 1987; Noegel et al., 1987; Wasenius et al., 1987), and dystrophin (Davison and Critchley, 1988; Koenig et al., 1988), the detailed composition of the motif in the 120-kD protein was distinctly different. Spectrin-like repeats are thought to be based on an α-helical coiled–coil structure. These repeats are characterized by a high alpha potential and a distinctive heptad repeat of hydrophobic residues and have little glycine and proline except in three small regions that are thought to correspond to linkers between the α-helical segments (Speicher and Marchesi, 1984). In contrast, the repeating motif in the 120-kD protein was rich in glycine and proline (Fig. 8) and showed no obvious heptad repeat. Moreover, the motif had a low alpha forming potential and instead showed a periodic variation in the prediction for extended or beta-like structure (Fig. 7 *A*) with a repeat distance of ~10 residues (Fig. 7 *B*). These differences in sequence and the differences in secondary structure would be consistent with the different appearance of electron micrographs of shadowed preparations of α-actinin and gelation factor (Condeelis et al., 1984). In these preparations, the gelation factor seemed to be more flexible than α-actinin and, in contrast to the uniform rod-like structure of α-actinin, gelation factor seemed to have a number of domains along its length which probably corresponded to the successive 100-residue motifs.

Close inspection of the 100-residue motif in the 120-kD gelation factor (Fig. 6 *B*) showed short zones rich in turn predictors such as proline, glycine, aspartic acid, and asparagine, alternating with zones with a high beta potential. Moreover, the high beta-potential zones often contained the characteristic HxHxHxH pattern in which hydrophobic residues were found in every second position often with hydrophilic residues filling the intervening positions (see Fig. 6 *B*). The centers of these high beta-potential HxHxH zones were spaced ~10 residues apart and correlated with the periodic variation of beta potential detected at this frequency by Fourier analysis. Although the alternation of the HxHxH high beta-potential zones with zones rich in turn predictors could be consistent with a beta barrel conformation, the regularity of the repeat suggested that it was probably more likely that each 100-residue motif in the 120-kD gelation factor has cross-beta conformation (that is, one in which the chains are aligned primarily perpendicular to the long axis of the molecule) with runs of probably about six to eight residues of sheet followed by two to four turn residues. Fig. 9 illustrates how such a structure could be built up, although clearly the model shown in this figure is only one of a number of related alternatives. Generally the cross-beta repeat seemed strongest in the center of the 100-residue motif and it could be that the structure at the ends of the motif was slightly different. In this structural model, the rod domain of the molecule would then be constructed from six cross-beta domains (*I–VI*, Fig. 9 *b*), each probably containing nine sheets arranged perpendicular to the long axis of the molecule. A structure like that shown in Fig. 9 would be analogous to that found in a number of other cross-beta structures. For example, *Chrysopa flavia* egg stalk silk (Geddes et al., 1968), scale (Stewart, 1977) and feather keratin (Fraser and MacRae, 1973, 1976), adenovirus fibers (Green et al., 1983), *Methanospirillum hungatei* sheath (Stewart et al., 1985), and silkworm chorion (Hamodrakas et al., 1988) all have similar short stretches of beta-sheet interspersed with turns. The length of the beta-sheet stretches varies somewhat between these examples, averaging three in the adenovirus fiber (Green et al., 1983) up to probably eight in *M. hungatei* (Stewart et al., 1985), and there is some uncertainty about the precise molecular conformation of the residues in the turns (discussed at length by Green et al., 1983). Support for this type of model has recently been obtained from circular dichroism studies which indicated an ellipticity of −2,600 degrees cm²/dmol at 218 nm and +4,300 degrees cm²/dmol at 195 nm, with zero ellipticity at 206 nm (Martin, S., P. M. Bayley, and M. Stewart, unpublished observations). These ellipticity values are consistent with a high content of beta structure and a low content of alpha structure in the gelation factor.

Because alternate residues in a beta sheet are directed above and below the plane of the sheet (see Fraser and MacRae, 1973), the HxHxH motif in the gelation factor would produce a sheet with one side hydrophobic and the other hydrophilic (Fig. 9 *d*). This suggests a simple mechanism to explain the dimerization of gelation factor subunits by way of joining the hydrophobic faces of the sheets deriving from each chain. Although there are clearly a number of different ways in which the chain could dimerize, model studies for the packing of beta sheets (Chou et al., 1986) are consistent with a model such as that illustrated in Fig. 9. Furthermore, such a model for the arrangement of the chains in the dimer would result in the hydrophilic faces of the 100-residue cross-beta domains facing outwards towards the solvent. Beta sheets in proteins tend to twist in a right-handed manner (Chothia, 1983; Chothia and Janin, 1981; Salemme, 1983). In the gelation factor rod, this would lead to a twisted double ribbon that would probably have approximate helical symmetry. Although the twist in beta sheets varies somewhat (Chothia, 1983; Salemme, 1983), most seem to be close to 20 degrees. Such a twist would produce a right-handed helix of pitch of ~8.5 nm, taking the axial spacing between chains in a cross-beta structure as 0.47 nm (Fraser and MacRae, 1973). Such a twist could possibly account for the modulation seen along gelation factor molecules in electron micrographs of shadowed material (Condeelis et al., 1984).

In Fig. 9 it has been assumed that the chains in the gelation factor molecule are arranged antiparallel and overlap by

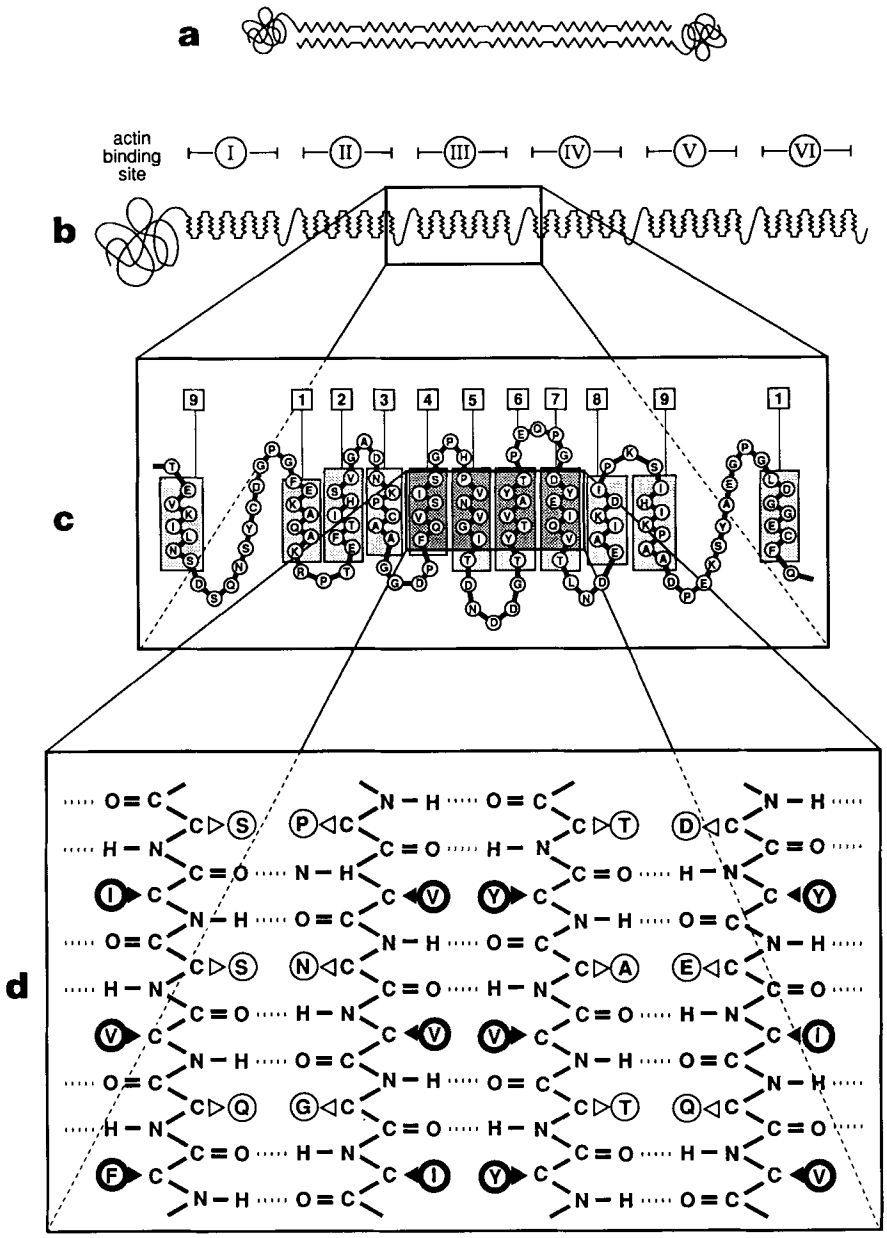

Figure 9. Highly schematic model of the way in which the amino acid sequence of the *Dictyostelium* gelation factor could be accommodated in a cross-beta configuration. Individual molecules of the gelation factor are composed of two antiparallel chains (*a*). Each chain (*b*) has an ~250-residue, putative actin binding site at its NH_2 terminus (shown as a globular domain) and six 100-residue repeats (*I–VI*) that constitute the rod domain of the molecule. Each 100-residue motif contains a series of short zones that have a high beta-forming potential alternating with several residues with a high potential for turns. The spacing between these zones is on the order of 10 residues. There are probably nine beta-rich zones in each motif, with ~10 residues forming a linkage between motifs. *c* shows a possible chain folding that would accommodate these features of the sequence in a cross-beta conformation for motif III. In this model there are nine runs of beta sheet, each of which is enclosed in a stippled box (*1–9*) (to give an idea of the continuity of the structure, sheet *9* of motif *II* and sheet *1* of motif *IV* are also shown). The precise position at which sheets and turns start and end is sometimes ambiguous and clearly the one illustrated is only one of several closely related structures. *d* shows a more detailed view of the residues in sheets *4–7*. Amino acid side chains that point upwards from the plane of the sheet are shown by filled triangles whereas side chains that are directed downwards are shown by open triangles. This illustrates how the HxHxH pattern, in which every second residue is hydrophobic, would give rise to a cross-beta sheet in which one side was hydrophobic. The joining of the hydrophobic faces of two chains would account for their dimerization in the molecule (*a*).

most of their length. An antiparallel arrangement is consistent with the appearance of electron micrographs of shadowed preparations of molecules labeled with monoclonal antibodies where two labeled sites related by a dyad axis are observed (Brink, M., M. Schleicher and G. Gerisch, unpublished observations). Although the precise degree of overlap has not been established, a complete overlap, such as that shown in Fig. 9, would appear most reasonable so that the interactions between motifs would be preserved. However, we cannot at this stage eliminate the possibility that each 100-residue unit folds into a compact structure, such as a beta barrel, and, if this were the case, it is possible that the molecules could interact only by their COOH termini and not have any substantial interactions between the 100-residue motifs. Although we think such a model less likely than models based on a cross-beta structure such as that in Fig. 9, clearly more work is required to establish the structure of the 100-residue motif unequivocally.

The model shown in Fig. 9 is consistent with the measured size parameters of the 120-kD gelation factor. The axial spacing between chains in a cross-beta structure is near 0.47 nm (Fraser and MacRae, 1973) and so each motif would measure ~4.3 nm axially. Thus, the six 100-residue domains in the gelation factor rod would have an axial extent of ~26 nm. The linkers between domains would increase the length, probably by 2–6 nm overall, and there would also be a contribution of several nanometers from the putative actin-binding domain. Therefore, the overall molecular length predicted from the model would probably be in the range of 30–40 nm, which is in agreement with the observed value of 35 nm (Condeelis et al., 1984). The spacing between residues along a chain in a beta sheet is ~0.35 nm (Fraser and MacRae, 1973) and so, if the chains in the beta sheets contained six residues, they would be ~2.1 nm wide. There would be some additional width due to the residues in the turns and so the molecular width predicted from the model

would be ~3 nm. The thickness of such a structure would probably be ~1.5 nm. If the sheets coiled around one another in a helical arrangement, the molecular width in electron micrographs would be between these values, but probably closer to the higher one. Thus the width predicted for the model is quite consistent with the 3 nm observed by electron microscopy (Condeelis et al., 1984).

Although clearly the structure of the rod portion of the 120-kD gelation factor needs to be investigated directly using such methods as electron microscopy and x-ray diffraction, the model we propose here seems to be consistent with both the amino acid sequence data and the physical dimensions of the molecule and so may serve as a working model until more definitive structural information is available.

We are most grateful to our colleagues in Cambridge and Martinsried, and in particular to Drs. G. Gerisch, H. Hartmann, A. D. McLachlan, J. Segall, and P. N. T. Unwin for their many helpful comments and criticisms. We also thank Drs. P. Bayley and S. Martin, of the National Institute for Medical Research, Mill Hill, UK, for assistance in recording CD spectra; Jürgen Enczmann and Christine Gurniak for help in the initial screening; Daniela Rieger for excellent technical assistance; Harald Kolmar for synthesis of oligonucleotides; and Annette Lenton for artwork. These sequence data are registered with the EMBL GenBank Nucleotide Databases under the accession number X15430.

This work was supported by grants No113/5 and Sch1204/2 from the Deutsche Forschungsgemeinschaft.

Received for publication 4 January 1989 and in revised form 4 April 1989.

References

André, E., F. Lottspeich, M. Schleicher, and A. Noegel. 1988. Severin, gelsolin, and villin share a homologous sequence in regions presumed to contain F-actin severing domains. *J. Biol. Chem.* 263:722-727.

Baron, M. D., M. D. Davison, P. Jones, and D. R. Critchley. 1987. The sequence of chicken α-actinin reveals homologies to spectrin and calmodulin. *J. Biol. Chem.* 36:17623-17629.

Brier, J., M. Fechheimer, J. Swanson, and D. L. Taylor. 1983. Abundance, relative gelation activity, and distribution of the 95,000-dalton actin-binding protein from *Dictyostelium discoideum*. *J. Cell Biol.* 97:178-185.

Carboni, J. M., and J. S. Condeelis. 1985. Ligand-induced changes in the location of actin, myosin, 95K (α-actinin), and 120K protein in amebae of *Dictyostelium discoideum*. *J. Cell Biol.* 100:1884-1893.

Chothia, C. 1983. Coiling of beta-pleated sheets. *J. Mol. Biol.* 163:107-117.

Chothia, C., and J. Janin. 1981. Relative orientation of close-packed beta-pleated sheets in proteins. *Proc. Natl. Acad. Sci. USA.* 78:4146-4150.

Chou, K.-C., G. Nemethy, S. Rumsey, R. W. Tuttle, and H. A. Scherga. 1986. Interactions between two beta-sheets: energetics of beta-beta packing. *J. Mol. Biol.* 188:641-649.

Chou, P. W., and G. D. Fasman. 1978. Empirical prediction of protein conformation. *Annu. Rev. Biochem.* 47:251-276.

Claviez, M., K. Pagh, H. Maruta, W. Baltes, P. Fisher, and G. Gerisch. 1982. Electron microscopic mapping of monoclonal antibodies on the tail region of *Dictyostelium* myosin. *EMBO (Eur. Mol. Biol. Organ.) J.* 1:1017-1022.

Condeelis, J., and M. Vahey. 1982. A calcium- and pH-regulated protein from *Dictyostelium discoideum* that cross-links actin filaments. *J. Cell Biol.* 94:466-471.

Condeelis, J., S. Geosits, and M. Vahey. 1982. Isolation of a new actin-binding protein from *Dictyostelium discoideum*. *Cell Motil.* 2:273-285.

Condeelis, J., J. Salisbury, and K. Fujiwara. 1981. A new protein that gels F-actin in the cell cortex of *Dictyostelium discoideum*. *Nature (Lond.).* 292:161-163.

Condeelis, J., M. Vahey, J. M. Carboni, J. DeMey, and S. Ogihara. 1984. Properties of the 120,000 and 95,000 dalton actin-binding proteins from *Dictyostelium discoideum* and their possible functions in assembling the cytoplasmic matrix. *J. Cell Biol.* 99(Suppl.):119s-126s.

Davison, M. D., and D. R. Critchley. 1988. α-Actinins and the DMD protein contain spectrin-like repeats. *Cell.* 52:159-160.

Emini, E. A., J. V. Hughes, D. S. Perlow, and J. Boger. 1985. Induction of hepatitis A virus-neutralizing antibody by a virus-specific synthetic peptide. *J. Virol.* 55:836-839.

Fechheimer, M., J. Brier, M. Rockwell, E. J. Luna, and D. L. Taylor. 1982. A calcium- and pH-regulated actin binding protein from D. discoideum. *Cell Motil.* 2:287-308.

Fraser, R. D. B., and T. P. MacRae. 1973. Conformation in Fibrous Proteins. Academic Press, New York. 628 pp.

Fraser, R. D. B., and T. P. MacRae. 1976. The molecular structure of feather keratin. *Proc. Interntl. Ornithol. Congr. Australian Acad. Sci.* Canberra, Australia. 16:443-451.

Garnier, J., D. J. Osguthorpe, and B. Robson. 1978. Analysis of the accuracy and implications of simple methods for predicting the secondary structure of globular proteins. *J. Mol. Biol.* 120:97-120.

Geddes, A. J., K. D. Parker, E. D. T. Atkins, and E. Beighton. 1968. Cross-beta conformation in proteins. *J. Mol. Biol.* 32:343-358.

Green, N. M., N. G. Wrigley, W. C. Russell, S. R. Martin, and A. D. McLachlan. 1983. Evidence for a repeating cross-beta sheet structure in the adenovirus fibre. *EMBO (Eur. Mol. Biol. Organ.) J.* 2:1357-1365.

Hammonds, R. G. 1987. Protein sequence of DMD gene is related to actin-binding domain of α-actinin. *Cell.* 51:1.

Hamodrakas, S. J., H. E. Bosshard, and C. N. Carlson. 1988. Structural models of the evolutionarily conserved central domain of silk-moth chorion proteins. *Protein Eng.* 2:201-207.

Henikoff, S. 1984. Unidirectional digestion with exonuclease III creates targeted breakpoints for DNA sequencing. *Gene (Amst.).* 28:351-359.

Imamura, M., T. Endo, M. Kuroda, T. Tanaka, and T. Masaki. 1988. Substructure and higher structure of chicken smooth muscle α-actinin molecule. *J. Biol. Chem.* 263:7800-7805.

Kaufmann, E., N. Geisler, and K. Weber. 1984. SDS-PAGE strongly overestimates the molecular masses of neurofilament proteins. *FEBS (Fed. Eur. Biochem. Soc.) Lett.* 170:81-84.

Koenig, M., A. P. Monaco, and L. M. Kunkel. 1988. The complete sequence of dystrophin predicts a rod-shaped cytoskeletal protein. *Cell.* 53:219-228.

Lacombe, M.-L., G. J. Podgorski, J. Franke, and R. H. Kessin. 1986. Molecular cloning and developmental expression of the cyclic nucleotide phosphodiesterase gene of *Dictyostelium discoideum*. *J. Biol. Chem.* 261:16811-16817.

Lee, G., N. Cowan, and M. Kirschner. 1988. The primary structure and heterogeneity of tau protein from mouse brain. *Science (Wash. DC).* 239:285-288.

Lipman, D. J., and W. R. Pearson. 1985. Rapid and sensitive protein similarity searches. *Science (Wash. DC).* 227:1435-1441.

Lottspeich, F. 1985. Microscale isocratic separation of phenylthiohydantoin amino acid derivatives. *J. Chromatogr.* 326:321-327.

MacLean-Flectcher, S., and T. D. Pollard. 1980. Viscometric analysis of the gelation of *Acanthamoeba* extracts and purification of two gelation factors. *J. Cell Biol.* 85:414-428.

Maizel, J. V., and R. P. Lenk. 1981. Enhanced graphic matrix analysis of nucleic acid and protein synthesis. *Proc. Natl. Acad. Sci. USA.* 78:7665-7667.

Maniatis, T., E. F. Fritsch, and J. Sambrook. 1982. Molecular Cloning: A Laboratory Manual. Cold Spring Harbor Laboratory, Cold Spring Harbor, NY. 545 pp.

McLachlan, A. D., and M. Stewart. 1976. The 14-fold periodicity in tropomyosin and the interaction with actin. *J. Mol. Biol.* 103:271-298.

Newell, P. C., A. Telser, and M. Sussman. 1969. Alternative developmental pathways determined by environmental conditions in the cellular slime mold *Dictyostelium discoideum*. *J. Bacteriol.* 100:763-768.

Noegel, A., and W. Witke. 1988. Inactivation of the α-actinin gene in *Dictyostelium*. *Dev. Genet.* 9:531-538.

Noegel, A., D. L. Welker, B. A. Metz, and K. L. Williams. 1985. Presence of nuclear associated plasmids in the lower eukaryote *Dictyostelium discoideum*. *J. Mol. Biol.* 185:447-450.

Noegel, A., W. Witke, and M. Schleicher. 1986. cDNA clones coding for α-actinin of *Dictyostelium discoideum*. *FEBS (Fed. Eur. Biochem. Soc.) Lett.* 204:107-109.

Noegel, A., W. Witke, and M. Schleicher. 1987. Calcium-sensitive non-muscle α-actinin contains EF-hand structures and highly conserved regions. *FEBS (Fed. Eur. Biochem. Soc.) Lett.* 221:391-396.

Pollard, T. D., and J. A. Cooper. 1986. Actin and actin-binding proteins. A critical evaluation of mechanisms and functions. *Annu. Rev. Biochem.* 55:987-1035.

Pollard, T. D., S. M. Thomas, and R. Niederman. 1974. Human platelet myosin. I. Purification by a rapid method applicable to other nonmuscle cells. *Anal. Biochem.* 60:258-266.

Salemme, F. R. 1983. Structural properties of protein beta-sheets. *Prog. Biophys. Mol. Biol.* 42:95-133.

Sanger, F., S. Nicklen, and A. R. Coulson. 1977. DNA sequencing with chain terminating inhibitors. *Proc. Natl. Acad. Sci. USA.* 74:5463-5468.

Scheel, J., K. Ziegelbauer, T. Kupke, B. M. Humbel, A. A. Noegel, G. Gerisch, and M. Schleicher. 1989. Hisactophilin, a histidine-rich actin-binding protein from *Dictyostelium discoideum*. *J. Biol. Chem.* 264:2832-2839.

Schleicher, M., E. André, H. Hartmann, and A. A. Noegel. 1988*a*. Actin-binding proteins are conserved from slime molds to man. *Dev. Genet.* 9:521-530.

Schleicher, M., G. Gerisch, and G. Isenberg. 1984. New actin-binding proteins from *Dictyostelium discoideum*. *EMBO (Eur. Mol. Biol. Organ.) J.* 3:2095-2100.

Schleicher, M., A. Noegel, T. Schwarz, E. Wallraff, M. Brink, J. Faix, G. Gerisch, and G. Isenberg. 1988*b*. A *Dictyostelium* mutant with severe defects in α-actinin: its characterization using cDNA probes and monoclonal antibodies. *J. Cell Sci.* 90:59-71.

Simon, M.-N., R. Mutzel, H. Mutzel, and M. Veron. 1988. Vectors for expression of truncated coding sequences in *Escherichia coli*. *Plasmid.* 19:94-102.

Sobue, K., K. Kanda, T. Tanaka, and N. Ueki. 1988. Caldesmon: a common actin-linked regulatory protein in the smooth muscle and nonmuscle contractile system. *J. Cell. Biochem.* 37:317–325.

Speicher, D. W. 1986. The present status of erythrocyte spectrin structure: the 106-residue repetitive structure is a basic feature of an entire class of proteins. *J. Cell. Biochem.* 30:245–259.

Speicher, D. W., and V. T. Marchesi. 1984. Erythrocyte spectrin is comprised of many homologous triple helical segments. *Nature (Lond.).* 311:177–180.

Spudich, J. A., and S. Watt. 1971. The regulation of rabbit skeletal muscle contraction. I. Biochemical studies on the interaction of the tropomyosin-troponin complex with actin and the proteolytic fragments of myosin. *J. Biol. Chem.* 246:4866–4871.

Stewart, M. 1977. The structure of chicken scale keratin. *J. Ultrastruct. Res.* 60:27–33.

Stewart, M. 1988. An introduction to the computer image processing of electron micrographs of 2-dimensionally ordered biological structures. *J. Electron Microsc. Technique.* 9:301–324.

Stewart, M., and A. D. McLachlan. 1975. 14 actin-binding sites on tropomyosin? *Nature (Lond.).* 257:331–333.

Stewart, M., T. J. Beveridge, and G. D. Sprott. 1985. Crystalline order to high resolution in the sheath of *Methanospirillum hungatei*: a cross-beta structure. *J. Mol. Biol.* 183:509–516.

Stewart, M., R. A. Quinlan, R. M. Moir, S. R. Clarke, and S. J. Atkinson. 1989. The role of repeating sequence motifs in interactions between α-helical coiled-coils such as myosin, tropomyosin and intermediate filament proteins. *In* Cytoskeletal and Extracellular Proteins: Structure, Interactions, and Assembly. U. Aebi and J. Engel, editors. Springer-Verlag, Heidelberg, FRG. 150–159.

Stossel, T. P., C. Chaponnier, R. M. Ezzell, J. H. Hartwig, P. A. Janmey, D. J. Kwiatkowski, S. E. Lind, D. B. Smith, F. S. Southwick, H. L. Yin, and K. S. Zaner. 1985. Nonmuscle actin-binding proteins. *Annu. Rev. Cell Biol.* 1:353–402.

Towbin, H., T. Staehelin, and J. Gordon. 1979. Electrophoretic transfer of proteins from polyacrylamide gels to nitrocellulose sheets: procedure and some applications. *Proc. Natl. Acad. Sci. USA.* 76:4350–4354.

Wallraff, E., M. Schleicher, M. Modersitzki, D. Rieger, G. Isenberg, and G. Gerisch. 1986. Selection of *Dictyostelium* mutants defective in cytoskeletal proteins: use of an antibody that binds to the ends of α-actinin rods. *EMBO (Eur. Mol. Biol. Organ.) J.* 5:61–67.

Warrick, H. M., and J. A. Spudich. 1988. Codon preference in *Dictyostelium discoideum*. *Nucleic Acids Res.* 16:6617–6635.

Wasenius, V.-M., O. Närvänen, V.-P. Lehto, and M. Saraste. 1987. α-Actinin and spectrin have common structural domains. *FEBS (Fed. Eur. Biochem. Soc.) Lett.* 221:73–76.

Witke, W., W. Nellen, and A. Noegel. 1987. Homologous recombination in the *Dictyostelium* α-actinin gene leads to an altered mRNA and lack of the protein. *EMBO (Eur. Mol. Biol. Organ.) J.* 6:4143–4148.

Witke, W., M. Schleicher, F. Lottspeich, and A. Noegel. 1986. Studies on the transcription, translation, and structure of α-actinin in *Dictyostelium discoideum*. *J. Cell Biol.* 103:969–975.

Yanisch-Perron, C., J. Vieira, and J. Messing. 1985. Improved M13 phage cloning vectors and host strains: nucleotide sequences of the M13mp18 and pUC19 vectors. *Gene (Amst.).* 33:103–119.

Young, R., and R. W. Davis. 1983. Efficient isolation of genes by using antibody probes. *Proc. Natl. Acad. Sci. USA.* 80:1194–1198.